Ablation and geometry change study of solid armature in a railgun*

Zhang Ya-Dong(张亚东), Ruan Jiang-Jun(阮江军), Hu Yuan-Chao(胡元潮), Gong Ruo-Han(龚若涵), and Wen Wu(文 武)†

School of Electrical Engineering, Wuhan University, Wuhan 430072, *China*

(Received 27 October 2012; revised manuscript received 29 December 2012)

Armature plays an important role in the electromagnetic launch process. Due to the skin effect, the current density distribution is neither uniform on the rail, nor on the armature. High current density centralization in one part could lead to a partial high temperature and make the armature material melt down and be ablated, especially at low velocity. In this paper we try to change the geometry of a Cshaped armature to improve the current density distribution and reduce the ablation. Four variants of C-shaped armatures are designed to study the specific features, including a conventional C-shaped armature (CCA), a rounded leading edge C-shaped armature (LCA), a rounded trailing edge C-shaped armature (TCA), and a rounded incorporate edge C-shaped armature (ICA). A novel low-speed experiment is constructed and tested. The armatures are ablated and recovered to compare the improved effects. Then finite element simulations according to the experimental results are performed to further analyze the experimental results. It is proved that the current density and hence the temperature distribution can be immensely improved by simply changing the armature geometry. LCA and ICA show that the erosion is more uniform on the contact surface due to the rounded leading edge. The curved trailing edge could improve the uniformity of the current on the interface. ICA which combines the effects of LCA and TCA is the best option in the four armatures. How much the leading edge and the trailing edge should be curved involves the geometry of CCA and the posture of the interface on the rail. A saddle shape is a good option to improve the current density and temperature distribution in the throat. Erosion mechanism is analyzed finally. The experiments and simulations support the erosion and transition mechanism. A detailed description of the experiments and simulations is also presented in this paper.

Keywords: railgun, ablation, friction, geometric modeling

PACS: 41.75.Lx, 85.70.Ay, 85.70.RP **DOI:** 10.1088/1674-1056/22/8/084102

1. Introduction

Significant progress has been made in the electromagnetic launch field in recent year. Erosion and transition have received more attention than ever before.[1–6] So far some factors influencing the erosion and transition have been universally received by researchers.

The amount of electrical erosion is to the first order linearly proportional to velocity and to current squared.[3] The quantity of material eroded increases substantially with current increasing, but less with velocity increasing. Reference [4] indicates that simple thermal vaporization is not likely to be responsible for the armature damage observed. The vaporization rate is sufficient to account for the total volume of armature material lost in the post-transition environment. However, it fails to explain the pattern of armature wear seen on recovered transitioned armatures. Thus, the post-transition interface is likely to be categorized by an arcing electrical contact. It was confirmed in Ref. [5] that mechanical wear is an important and possibly dominant contributor to wear at high velocity. However, at low velocity (< 1 km/s), mechanical wear is small compared with electrical wear. High current density centralization in one part could lead to a high partial temperature and make the rail and armature material melt down and become eroded. According to the above opinions, no matter whether the armature damage is due to erosion or transition (including thermal vaporization and arcing electrical contact), it is associated with current, especially at low velocity. Since the heat deposited varies with the square of the current density, a small reduction in current density will result in a larger reduction in temperature.

Armatures play an important role in the electromagnetic launch process. To reduce erosion and transition, the geometry and materials used for the armature have been changed to improve the current distribution.[7–11] Generally speaking, geometry change is a practical and effective method. The conventional C-shaped armature (CCA) is widely used, which experiences high current densities in three areas: the leading edge, the trailing edge, and the throat. It is argued that if the armature shape is modified to better align with the magnetic field, the current density distribution could be more uniform.

In this paper, we try to analyze the ablation and geometry change on a C-shaped armature at low velocity. Four variants of C-shaped armatures are designed to study the specific features, including a CCA, a rounded leading edge C-shaped armature (LCA), a rounded trailing edge C-shaped armature (TCA), and a rounded incorporate edge C-shaped armature (ICA). A novel low-speed experiment is constructed and tested

*Project supported by the National Basic Research Program of China (Grant No. 2011CB209404) and the Post-doctoral Science Foundation of China (Grant No. 2012M521465).

†Corresponding author. E-mail: wenwu654321@163.com

© 2013 Chinese Physical Society and IOP Publishing Ltd

for these specific features incorporated into C-shaped armatures. The armatures are eroded and recovered to compare the improved effects. Then finite element simulations according to the experiment are performed to analyze the results. The geometry change on a C-shaped armature will be useful for the ablation studues.

2. Experiment design of the railgun

2.1. Design of the experiment

The equivalent circuit of a basic capacitor-driven railgun is shown in Fig. 1.

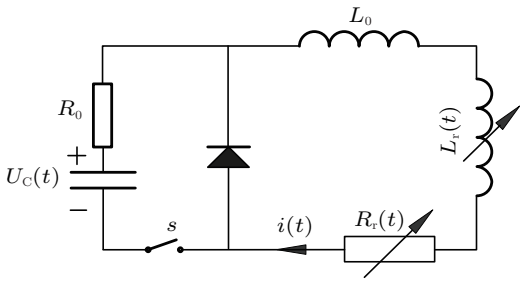


Fig. 1. The equivalent circuit of a basic capacitor-driven railgun.

In Fig. 1, L_r and R_r are the inductance and resistance of the railgun respectively; L is the pulse forming inductance. According to the basic railgun equation, the magnetic propulsive force in the canal-direction can be expressed as

$$F = \frac{1}{2} L_r' I^2 = ma, \tag{1}$$

where, L_r' is the inductance gradient value of the railgun.

The propulsive force does correspond to the high-frequency limit of the inductance gradient in the absence of any containment structure.[9,10] In the two-dimensional (2D) finite element simulation the value of L_r' is taken to be 0.5 μH/m at 1000 Hz based on the experiment. We use this value to design the system.

For the low velocity study, generally speaking, 100 m/s is selected as a lower limit, below which the velocity skin effect (VSE) starts to become negligible.[3] In order to observe the current influence on erosion alone, a small power source is used to drive the armature which could eliminate the effect of the VSE. The velocities of the armatures are controlled around 40 m/s in the experiment.

Friction of the armature cannot be ignored compared with the small propulsion. Preloading force added to the rail is crucial in the experiment which relates to the friction. If the preloading force is too big, the static friction will be big enough to prevent the armature from moving in the bore. The armature and the rail are contacted with each other so well it is as if no erosion appears on the contact surface at all. On the contrary, if the preloading force is too small, most of the system energy will transfer to the arc between the armature and the rail. The armature cannot move out of the bore and the contact surface will be eroded very unevenly. A drill autofeeder is built to measure the static force which could give a slow but steady force acting on the armature. The experiment shows that the best static friction we tested is almost 35 N∼40 N, which can make the armature shoot out of the muzzle easily and the contact surface of the armature will be evenly eroded. A typical measurement of the maximum static friction force is shown in Fig. 2 in which a division on the vertical axis is 20 N.

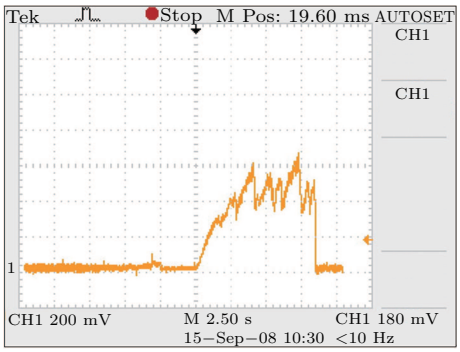


Fig. 2. (color online) Measurement of the maximum static friction force.

Kinetic friction force also must be concerned about in the experiment, especially when the railgun is energized. The polarity and magnitude of the current will influence the friction effect for various metals.[12–14] Tribological behavior and surface temperature of the brass greatly depend on current density. The increase of current results in an increase in surface temperature and mass loss of brass and decrease in friction coefficient of the couple. Current density has a better effect on surface temperature at low velocity specially. Electrical arc corrosion exists on the worn surface.[14] When the temperature is above 100 K, the friction coefficient decreases with temperature.[15] It is really difficult to give an accurate expression for railgun friction which includes current, temperature, mass, and other factors. In Ref. [16] a simple equation was suggested for the solid friction in a railgun. The friction coefficient could be written as

$$\mu(v) = (\mu_H - \mu_G)\, e^{-av} + \mu_G, \tag{2}$$

where μ_H and μ_G are static and kinetic friction coefficient and a is the attenuation coefficient. Detailed parameters were used as shown in Ref. [17], where $\mu_H = 0.14$, $\mu_G = 0.1$, and $a = 0.05$. Figure 3 shows that the friction coefficient varies rapidly with the speed of the armature increasing in a range of 0–50 m/s. The simulation result is identical to the experimental result as shown in Fig. 4. The current peak value is almost 23 kA. The peak value of the propulsion is almost 130 N.

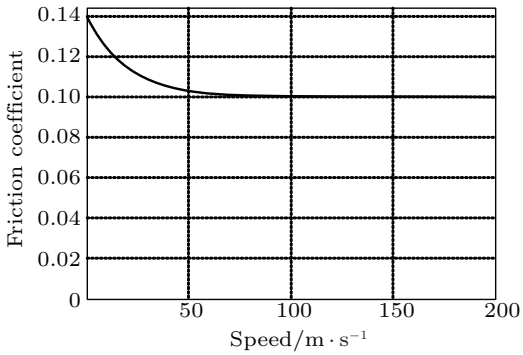


Fig. 3. Friction coefficient varying with the velocity of the armature.

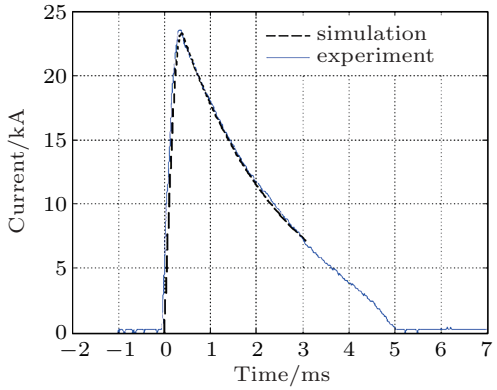
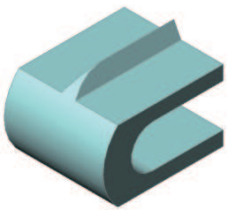
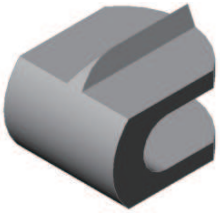


Fig. 4. (color online) Current curves obtained from the railgun simulation and experiment.

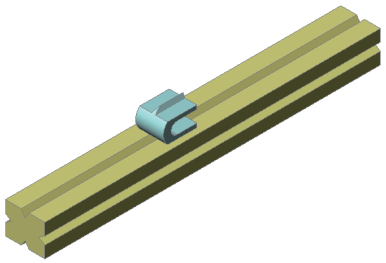
2.2. Design of the armatures

Due to the small propulsion and uneven friction, the armature may become stumbled or even stuck in the bore. So we add two "wings" to the armature and use triangular ditched rail to guide the armature moving along the bore line. The experimental installation and the visual image of the typical rail and armature (CCA) are shown in Fig. 5.

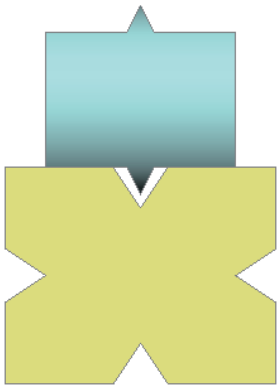
Table 1. (color online) Four types of C-shaped armatures.

	
conventional C-shaped armature (CCA)	rounded leading edge C-shaped armature (LCA)
	
rounded trailing edge C-shaped armature (TCA)	rounded incorporate edge C-shaped armature (ICA)

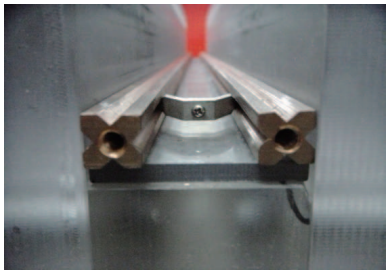
Four types of C-shaped armatures are designed to compare the effects of geometry change including CCA, LCA, TCA, and ICA which are shown in Table. 1.



(a) Oblique view



(b) front view



(c) experimental railgun with a solid V-shaped laminated armature

Fig. 5. (color online) The armature and the triangular ditched rail.

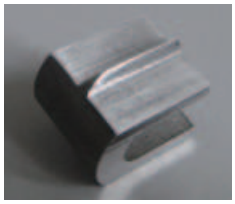
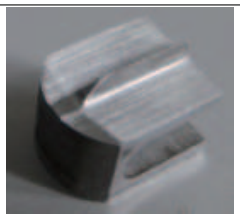
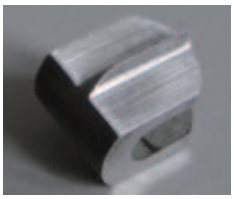
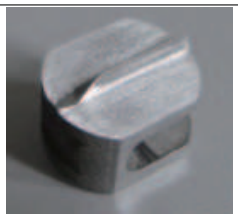
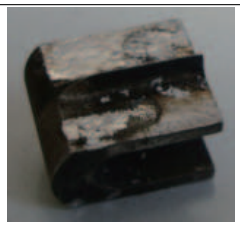
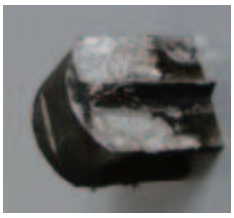
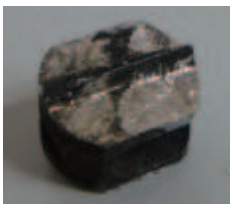
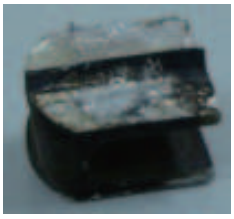
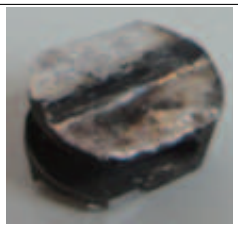
The saddle-shaped throat armature is not considered here because the throat cannot be eroded under the small current and no effect of the geometry change on it is found. Typical eroded armatures are shown in the second and third row of Table 2.

3. Finite element simulations and analysis

3.1. Loading current

The variations of the simulation result of the current and velocity with displacement of the armature are shown in Fig. 6. We can see that the current increases quickly at the initial position where the velocity of the armature is quite small. Then, the current reduces slowly from the peak value with displacement increasing. Most of current energy is consumed at the very beginning of the armature motion. It means that erosion may occur at the initial position of the armature which is almost at 0.35 ms.

Table 2. (color online) Erosion pictures of the four different armatures.

	CCA	LCA	TCA	ICA
Original model				
Typical test No. 1				
Typical test No. 3				

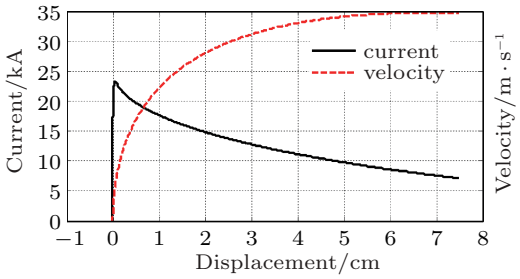


Fig. 6. (color online) Variations of current and velocity with displacement.

What we are concerned about is the influence of the current on erosion. Due to the skin effect, the current density distribution is not uniform on the rail nor on the armature, we need to perform three-dimensional (3D) analysis in order to calculate it accurately. Under the assumption of the nondisjunction and ideal entire contact between the armature and rail, stationary finite element analyses are performed on various armatures by an ANSYS code. According to the method in Ref. [11], current density distribution and consequently the temperature field distribution characteristics in the armature are simulated with a peak current of 23 kA from 0 to 0.35 ms.

3.2. Maximum current density on the whole armature

The simulation results of current and temperature of the armatures at 0.35 ms are summarized in Table 3. As shown in the second to the sixth row of Table 3, the maximal values of the current density and joule heat appear at point "*a*" in CCA, "*b*" in LCA, "*c*" in TCA, and "*d*" in ICA respectively. Compared with the maximum value of CCA, no matter whether the leading edge or the trailing edge is curved or not the current density of the armature can be reduced, which are shown in the seventh and eighth row.

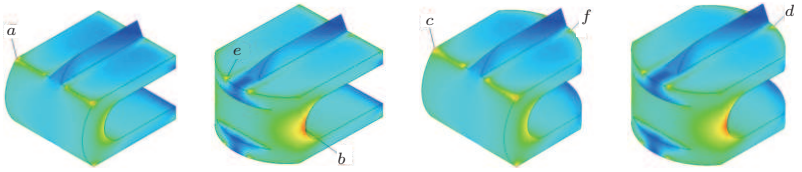
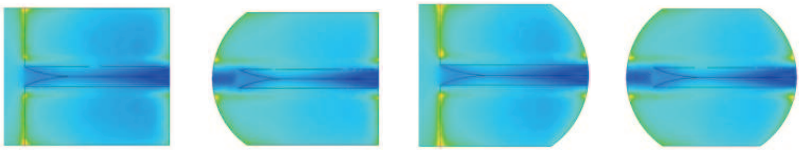
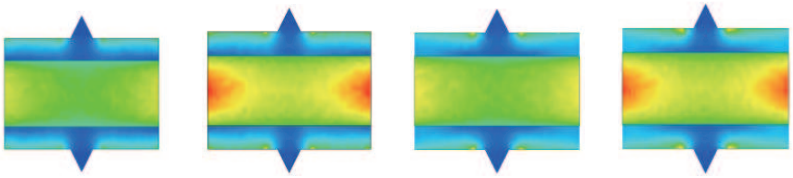
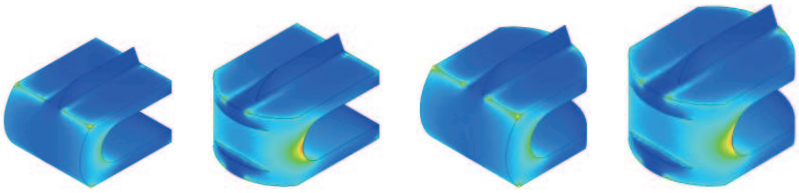
The position of the maximum current density will change from the surface of the armature to the throat with the variation of the radius of the rounded leading edge. As shown in the second, fourth, and fifth row, we can see that the throat suffers great current especially in the internal and lateral corner. The leading edges in LCA and ICA are curved which leads to the reduced volume of the throat and an increase of the current density and joule heat. It can be concluded that if the current loaded on the rail launcher is very big, the throat must be eroded. To improve the erosion, throats of the LCA and ICA should be modified into the saddle shape as indicated in Refs. [7]–[10], which increases the volumes of the internal and lateral throat and fits the distribution of the current.

3.3. Erosion on the interface of armature

According to the simulation results in the ninth to the twelfth row of Table 3, no matter whether the leading edge or the trailing edge is curved or not, the current density on the contact surface can be reduced. The experimental results consist with the simulation results. The ablation of CCA is deeper and more uneven than those of other armatures as shown in Table 2. The fore part of the armature is eroded greatly. A pit is seen on points "*e*" and "*a*". The rear part of the armature has little erosion, which is shown in Fig. 7.

The effect of LCA is very remarkable and can reduce the maximum current density greatly at the leading edge. The point of the maximum current density at the leading edge changed from "*a*" to "*e*". A slight layer on the interface of

Table 3. (color online) Simulation results of the four armatures.

		CCA	LCA	TCA	ICA
Three-view drawing of the current density distribution	Location of the maximum current density distribution oblique view				
	Front view				
	Side view				
	Dorsal view				
Three view drawing of the joule heat distribution	Oblique view				
In the whole armature	Maximum current density/10^9 A·m^{-2}	1.7561	1.2056	1.5155	1.3086
	Maximum joule heat/10^{10} J	8.9438	4.2153	6.6602	4.9662
On the leading edge	Maximum current density/10^9 A·m^{-2}	1.7561	1.1948	1.5155	1.1621
	Maximum joule heat/10^{10} J	8.9438	4.1396	6.6602	3.9167
On the trailing edge	Maximum current density/10^9 A·m^{-2}	1.0381	1.0537	1.2646	1.3086
	Maximum joule heat/10^{10} J	3.1252	3.2201	4.6379	4.9662

LCA is ablated uniformly. The trailing edge has little improvement, which can be seen in Fig. 8. It means that the angle of curve at the leading edge will influence the current distribution greatly. It is feasible to design an LCA whose points "*a*" and "*e*" have the same current density to restrict the heat in the contact surface.

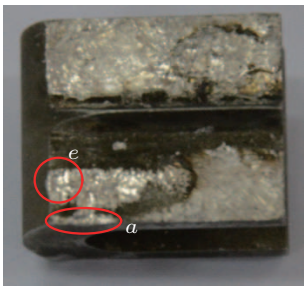


Fig. 7. (color online) Erosion pictures of the CCA.

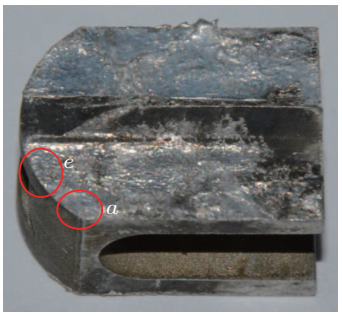


Fig. 8. (color online) Erosion pictures of the CCA.

The maximum current density of TCA reduces at the leading edge, but increases at the trailing edge, which can be seen in Fig. 9. The effect of TCA is not so good as that of LCA. However, the current density of the whole contour and interface will be more uniform than those in the case of CCA.

Table 2 shows that erosion of the whole interface of TCA is uniform although a bit deeper.

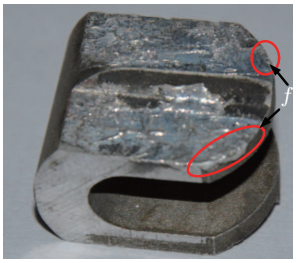


Fig. 9. (color online) Erosion picture of the TCA.

In the ICA, the point of the maximum current density changes from "*a*" to "*d*" which combines the effects of LCA and TCA. The value of the maximum current density will be reduced at the leading edge and increased at the trailing edge. The fore and rear parts of ICA are ablated heavily but the middle part was eroded slightly as indicated in Fig. 10 which is in accordance with the simulation.

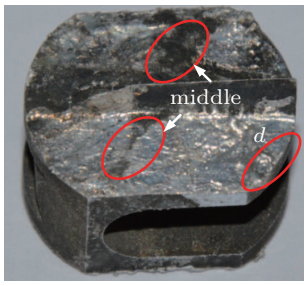


Fig. 10. (color online) Erosion pictures of the ICA.

This phenomenon can support the erosion and transition mechanism about "melt wave" behavior in this sense. According to this view, intense skin-effect heating leads to localized melting and loss of aluminum at the perimeter of the rail/armature interface. An erosion front progresses toward the center of the armature until localized magnetic forces cause the armature to separate from the rail. Meanwhile according to the erosion armatures of CCA and LCA, another wear mechanism, viscous heating, is also in operation. A thin film of molten aluminum at the sliding interface is sustained by intense viscous dissipation which made the middle part of the armature eroded before the trailing edge erosion. The ICA results validate the two wear theories.

What more attention should be paid to is that the maximum current density of ICA is greater than that of LCA. It means that how much the leading edge and the trailing edge should be curved involves the concerned geometry of CCA and the posture of the interface on the rail.

4. Conclusions

Four variants of C-shaped armatures are designed to study the geometry change on C-shaped armature at low velocity. A novel low-speed experiment is constructed and tested. The armatures are eroded and recovered to compare the improved effects. Then finite element analyses according to the experimental results are performed to further analyze the results. Conclusions drawn from the present study in the paper could provide guidelines for practice.

It is proved that even though we have not yet well optimized the armature geometry, it can be concluded from the experiments and simulations that the current density and hence the temperature distribution can be immensely changed by simply changing the armature geometry. LCA and ICA show less erosion on the contact surface due to the rounded leading edge. The curved trailing edge could improve the uniformity of the current on the interface. ICA is the best option in the four armatures, which combines the effects of LCA and TCA. How much the leading edge and the trailing edge should be curved involves the geometry of CCA and the posture of the interface on the rail.

Further finite-element analyses show that the method of the curved leading edge in this paper must be modified to better align with the magnetic field. It can be concluded from the simulation results that saddle shape is a good option to improve the current density and temperature distribution in the throat.

Finally, the experiments and simulations support the erosion and transition mechanism. It is seemed that two wear theories, "melt wave" behavior and viscous heating, are both workable.

References

[1] Wang Y, Richard A M and Cheng S K 2004 *Physics of Electric Launch* (Beijing: Science Press) p. 63
[2] Harry D F 2007 *IEEE Trans. Magn.* **43** 93
[3] Trevor W and Francis S 2005 *IEEE Trans. Magn.* **41** 448
[4] Andrew J P 2010 *Report in Army Research Laboratory*. "Stefan Model of the Post-transition Plasma Environment Encountered in Solid Armature Railguns"
[5] Francis S and Jerry V P 1999 *IEEE Trans. Magn.* **35** 100
[6] Xiao Z 2012 *Friction and Wear Behavior of Armature-Rail Sliding Electrical Contact Surface* Ph. D dissertation (Wuhan: Huazhong University of Science & Technology) (in Chinese)
[7] Sikhanda S, Trevor W and Chadee P 2007 *IEEE Trans. Magn*. **39** 408
[8] Laura R, Sikhanda S and Kuo T H 2003 *IEEE Trans. Magn.* **39** 72
[9] Dwight L and Sikhanda S 2007 *IEEE Trans. Magn.* **43** 150
[10] Bok k K and Kuo T H 1999 *IEEE Trans. Magn.* **35** 413
[11] Cao Z J 2006 *Characteristic Studies of C-shaped Solid Armatures in Electromagnetic Launch* MS dissertation (Wuhan: Huazhong University of Science & Technology) (in Chinese)
[12] Metal Physics Teaching and Research Section, Department of Physics, Jilin University 1959 *Acta Phys. Sin.* **15** 145 (in Chinese)
[13] Hu H F, Ji Y, Hu Y, Ding X Y, Liu X W, Guo J H, Wang X L and Zhai H C 2011 *Chin. Phys. B* **20** 044204
[14] Shangguan B, Zhang Y Z, Xing J D, Sun L M, Qiu M, Niu Y P and Hou M 2008 *The Chinese Journal of Nonferrous Metals* **18** 1237 (in Chinese)
[15] Wang Y Z, Huang P and Gong Z L 2012 *Acta Phys. Sin.* **61** 063203 (in Chinese)
[16] Aigner S and Igenbergs E B 1989 *IEEE Trans. Magn.* **25** 33
[17] Pascale L, Hilmar P and Joseph W 1993 *IEEE Trans. Magn.* **29** 848